J. Electrochem. Sci. Eng. **14(3)** (2024) 395-416; http://dx.doi.org/10.5599/jese.2351

Open Access : : ISSN 1847-9286
www.jESE-online.org

Original scientific paper

Strategy on enhancing ionic conductivity of biocompatible hydroxypropyl methyl cellulose/polyethylene glycol polymer blend electrolyte with TiO_2 nanofillers and $LiNO_3$ ionic salt

Mohan Srinivas and Rajashekhar F. Bhajantri✉

Department of Physics, Karnatak University, Dharwad 580003, Karnataka, India

Corresponding author: ✉rfbhajantri@kud.ac.in; Phone: +91-836-2215316(O); Mobile: +91 9448623319

Received: April 20, 2024; Accepted: June 9, 2024; Published: June 26, 2024

Abstract

A biocompatible and biodegradable polymer in the fabrication of solid polymer electrolytes for high energy density rechargeable batteries is gaining interest owing to their safety, compatibility and flexibility. In this study, a polymer electrolyte based on hydroxypropyl methylcellulose (HPMC)/polyethylene glycol (PEG) biopolymers, incorporating TiO_2 nanofillers and $LiNO_3$ as a lithium source, was fabricated using the solution casting method. Mixed-phase TiO_2 nanofillers were synthesized via hydrolysis of titanium tetraisopropoxide. The crystal structure, phase morphology, and electrochemical impedance spectra of the films and nanofillers were investigated. X-ray diffraction analysis confirmed the amorphous nature of the polymer electrolyte and crystalline nature of nanofiller. In addition, it was noted that the amorphous phase of the polymer blend remained unaltered despite the incorporation of TiO_2 and $LiNO_3$. Thermogravimetric analysis and differential thermal analysis confirmed that the pure blend exhibited a melting point of around 60°C and complete degradation of around 340 °C, while the blend electrolyte with additives demonstrated thermal stability with a broad melting point. The blend containing 5 wt.% TiO_2 fillers and 10 wt.% $LiNO_3$ionic salt exhibited the highest ionic conductivity of 0.213 mS cm^{-1} at room temperature. The polymer blend electrolyte displayed a narrow electrochemical stability window of 2.85 V, with the highest cationic transfer number of 0.323. The temperature-dependent ionic conductivity of the prepared polymer blend electrolyte followed Arrhenius behaviour, with an activation energy of 0.1 eV. The study examined and reported the effect of aging on the interfacial resistance of polymer blend electrolyte. The mechanical properties of the optimized HPMC/PEG/TiO_2/$LiNO_3$ polymer blend electrolyte were investigated and reported. Thus, this research elucidated the role of nanofillers and ionic salt in enhancing the performance of biocompatible polymer electrolytes.

Keywords

Mixed polymer; polymer composite; Arrhenius behaviour; cationic transference number; electrochemical stability

Introduction

The world's growing population and economic demands have led to a significant rise in global energy consumption. To meet the current energy needs of the world, it is imperative to engage in the mass production of energy [1]. However, relying solely on non-renewable sources like nuclear power plants, coal, and fossil fuels, as well as renewable resources like solar, wind, and hydroelectric power, is insufficient to fulfil the energy requirements of today. Moreover, the extraction of energy from non-renewable sources has contributed to the alarming global threats of global warming and pollution [2]. The effective resolution for these concerns lies in efficiently harnessing energy from sustainable and eco-friendly sources. The primary obstacle in maximizing energy extraction from environmentally friendly sources is the storage of the harnessed energy [3]. From the perspective of energy storage, new-generation energy storage devices with maximum energy density are investigated.

New generation supercapacitors and batteries with higher power and energy density gained much interest. In case of rechargeable batteries, the overall performance is not solely dependent on electrodes but also on the electrolytes within the cell. These electrolytes play a crucial role in achieving higher battery energy density [4]. The electrolytes can be in the form of liquid, gel, or solid, with liquid electrolytes offering certain advantages such as good wettability with electrodes, ionic conductivity, and reduced dendrite formation [5]. However, they are more susceptible to vulnerabilities and suffer significant drawbacks due to safety concerns, environmental issues, and limited energy density than solid electrolytes [6]. On the other hand, gel electrolytes composed of liquid components and polymer matrix have emerged as a promising alternative to liquid electrolytes, offering good heat resistance, higher ionic conductivity, and a stable electrode-electrolyte interface. The gel polymer electrolytes also offer electrode protection and control of the thermal runaway [7]. Nonetheless, the mechanical integrity of the cell remains a major drawback for gel electrolytes. Additionally, the presence of liquid fails to suppress dendrite formation [8]. In order to attain favourable mechanical cell integrity and interfacial properties, the solid polymer composite appears to be a viable option. Typically, solid polymer electrolytes (SPE) composed of polymer chains exhibit flexibility and integrity, providing a range of adjustable parameters alongside excellent thermal stability and ionic conductivity [9].

The low-flammable solid polymer electrolyte has major restrictions based on the nanocomposite and the host polymer matrix. Brittle ceramic electrolytes exhibit lower ionic conductivity at room temperature, whereas sulphide electrolytes exhibit poor stability but higher conductivity. The polymer electrolyte made of host polymer matrix usually includes polyvinylidene fluoride (PVDF), polyethylene oxide (PEO), polyvinyl alcohol (PVA) and several polymer blends like PEO-methylcellulose (MC), PVDF-hexafluoropropylene (HFP), *etc*. [10]. Among numerous polymer blends like PEO-carboxyl methyl cellulose (CMC), PVA-sodium alginate (SA) and PEO-polyvinyl pyrrolidone (PVP) [11], the blending of crystalline polymer with amorphous one gains tremendous interest. PEO and PVDF-co-hexafluoro-propylene (HFP) polymer matrix with active nanofillers have been widely studied as electrolytes. The enhanced ionic conductivity observed in PVDF-HFP is attributed to the reduction in crystallinity of PVDF with the addition of amorphous HFP, while the blending of PEO with methylcellulose(MC)/ /polyvinyl chloride (PVC) yields better ionic conductivity and good mechanical properties [12,13]. The dielectric oxide ceramics embedded in polymers make solid electrolytes appear as potential candidates due to their affordability and demonstrated ability to offer increased power density, flexibility, and improved ionic conductivity. Furthermore, including active oxide fillers in the polymer composite improves ionic conductivity and increases the ion transference number and wider electrochemical stability window [14]. The ionic conductivity, along with the electrochemical window

and thermal stability, can further be increased by the addition of ionic liquids along with oxide fillers, which have to be optimized. The increase in ionic conductivity can be attributed to the dissociation of ions resulting from Lewis acid-base interactions between the anions of ionic species and the surface groups of polymer chains containing nanofillers [15]. Most widely studied passive inorganic oxide fillers include TiO_2, ZnO, MgO, Al_2O_3, CeO_2, $BaTiO_3$ and SiO_2, while the active fillers based on Li include$Li_7La_3Zr_2O_{12}$ (LLZO), $Li_{6.4}La_3Zr_{1.4}Ta_{0.6}O_{12}$ (LLZTO) and $Li_{0.29}La_{0.57}TiO_3$ (LLTO) [9,15]. For active fillers, higher interfacial resistance, poor compatibility with electrodes, and comparatively higher dendrite formation limit their commercialization [16]. Additionally, these passive fillers reduce the crystallization of the polymer matrix, simultaneously enhancing the channels for ion migration [9].

A water-soluble semi-synthetic hydroxypropyl methylcellulose (HPMC) is a nonionic cellulose amorphous polymer with a molecular formula ($C_{56}H_{108}O_{30}$), derived from polysaccharide units of plant cells through etherification of cellulose in which the hydroxyl groups are replaced by hydroxy propyl and methyl groups [17]. The presence of functional groups made HPMC thermo-sensitive with water retention capabilities. Biodegradable and biocompatible HPMC found applications in moderate coatings, tablet binders, drug delivery, adhesives, agriculture and cosmetics [18]. A synthetic non-immunogenic polyether (PEO), which is based on molecular weight and called also polyethylene glycol (PEG), is a semi-crystalline polymer. Moreover, PEG is a linear water-soluble polymer with molecular formula $HO(CH_2CH_2O)_nH$, and it is widely used in many biomedical, pharmaceutical, and industrial applications. PEG is also broadly used in tissue engineering and drug delivery systems due to its biocompatibility. PEG offers good film flexibility, tensile strength and barrier properties in addition to phase partitioning [19].

An extensive study has already been conducted on inorganic passive TiO_2 fillers in polymer matrix due to their good thermal stability and chemical inertness properties [15,20]. The nano TiO_2 has gained tremendous interest due to its non-toxicity, chemical inertness and optical energy band gap [21]. Also, TiO_2 has excellent mechanical, thermal and chemical properties and favours the formation of minute crystallites, thus reducing the crystallization of polymer, consequently providing new pathways for the migration of ions and charge carriers through the polymer ceramic interface [22]. Further, few surveys have reported that just the shapes of nanomaterial in the polymer blend/host polymer matrix enhance ionic conductivity. The nanomaterial with rod/wire structure exhibits excellent electrochemical properties over the spherical-shaped nanomaterial [23]. Moreover, some studies have also reported that modification of the surface of TiO_2 rods, or oxygen-induced structural modification, exhibits a good interfacial interface and enhanced ionic conductivity [16]. The defect-induced 1D nano TiO_2 micro rods developed by Luo *et al*. reported that the addition of TiO_2 micro rods into the PEO matrix not only reduces the crystalline phase but also improves the interfacial region with electrodes [16]. Li *et al.* reported that TiO_2 forming large surface area nanowires and length-diameter ratio doped with Ti^{3+} ions in PEO polymer exhibit enhanced Li-ion conductivity of the order 10 mS cm^{-1} [23]. Furthermore, an excellent electrochemical stability window of 5.5 V at 60 °C, and a higher Li transport number of 0.36 was achieved. The addition of TiO_2 into PVDF-co-HFP reduces the porousness of the electrolyte while enhancing the ionic conductivity and interfacial stability, as reported by Ramaiah *et al.* [24].

Rechargeable Li-ion batteries have gained the interest of worldwide researchers due to the standard lithium reduction potential of -3.04 V (*vs*. SHE) and outstanding reversible electrochemical efficiency with theoretical specific capacity of 3860 mAh g^{-1}, long life, and easy intercalation of smaller Li ions compared to other ions [25]. As Li-ion source is not abundant, its reactivity with the environment and high risk of short circuits due to dendrite formation encourages researchers to find a new

alternative with the same efficiency and performance [10]. In this perspective, sodium and magnesium ion batteries emerge as possible alternatives to Li-ion batteries. Nevertheless, the movement of Na and Mg ions is slow due to their sluggish behaviour and larger ionic size. Additionally, the energy density of these batteries is comparatively lower than that of Li-ion batteries [26].

Herein, we report the synthesis of nano TiO_2 particles *via* hydrolysis of titanium tetra-isopropoxide. To the best of our knowledge, the biocompatible hybrid nano ceramic polymer composite made of polymer blend HPMC/PEG with the addition of $LiNO_3$ salt and TiO_2 filler has not been previously reported. The effect of TiO_2 and $LiNO_3$ applied as filler and ionic salt on structural, electrical and mechanical properties of HPMC/PEG/TiO_2/$LiNO_3$ polymer blend electrolyte has been systematically investigated. The ionic conductivity, the interaction of the polymer with filler, cationic transfer number, electrochemical stability window, and mechanical tensile strength of the optimized HPMC/ /PEG/TiO_2/$LiNO_3$ polymer blend electrolyte have been evaluated and reported.

Experimental

Chemicals

Titanium tetra-isopropoxide(Assay 98 %, Spectrochem, India), nitric acid (HNO_3, AR, SD-Fine Chem, India), hydroxypropyl methylcellulose (HPMC, methoxy content:28 to 30 %, hydroxy content: 7 to 12 %, SD-dine chem, India), polyethylene glycol 6000 (PEG, 98 %, Spectrochem, India), lithium nitrate (AR grade, 98 %, Loba Chemie Pvt. Ltd, India) were used in the present study without any further purification. Distilled water is used as a solvent throughout the experiment.

Synthesis of TiO_2

TiO_2 nanoparticles were synthesized by controlled hydrolysis of titanium tetraisopropoxide (TTIP). A 50 ml of TTIP was taken in a dry beaker, and another 50 ml of double distilled water was slowly added dropwise to the TTIP solution under continuous stirring. pH was adjusted using 1:1 HNO_3, which was added slowly while continuously monitoring the pH. Upon adding distilled water, the white precipitate of titanium hydroxide was formed and vacuum filtered using Whatman filter paper, which was washed several times with distilled water [27]. The filtrate was dried at 100 °C for 15 hours in a hot air oven. The obtained powder was finely grounded using an agate mortar and placed in a muffle furnace at 300 °C for 3 hours in the air to remove any residual content [27]. The calcined TiO_2 powder was characterized and used as a nano-filler in polymer electrolytes.

Fabrication of HPMC/PEG/TiO_2/$LiNO_3$ polymer blend electrolytes

The circular polymer film of 100 mm diameter was prepared by the standard solution casting technique. Initially, the blends of HPMC(100-x)/PEG(x), (x = 25 to 60 wt.%)were prepared by dissolving stoichiometric weights of HPMC and PEG 6000 polymers in distilled water. The colloidal solution was then stirred for around 400 rpm at room temperature for 16 hours to obtain a homogeneous mixture. The HPMC/PEG mixed solution was then sonicated at 15 kHz for 10 min to get the uniform electrolyte slurry. Finally, the slurry was cast onto plastic Petri dishes and dried in a hot air oven for 24 hours at 50 °C. The polymer films of around 50-100 µm thickness were obtained for different compositions of HPMC/PEG. Further, the films were stored in a zip lock cover under a vacuum and subjected to electrochemical studies.

Nano TiO_2 particles were introduced into the polymer blend by taking HPMC/PEG/(y)TiO_2 (y =1, 2, 5, 10 wt.%), stirred at 500 rpm for 18 h, and solution casted as mentioned above. After optimizing HPMC/PEG/TiO_2 films, a white colour, HPMC/PEG/TiO_2/$LiNO_3$ (polymer composite) films of

thickness 120-175 µm were made by the addition of $LiNO_3$salt up to 15 wt.%, keeping 5 wt.% of titanium oxide constants. The schematic representation of a polymer composite containing TiO_2 and $LiNO_3$ and the interaction of polymer chains with nanofillers and Li ions is shown in Figure 1.

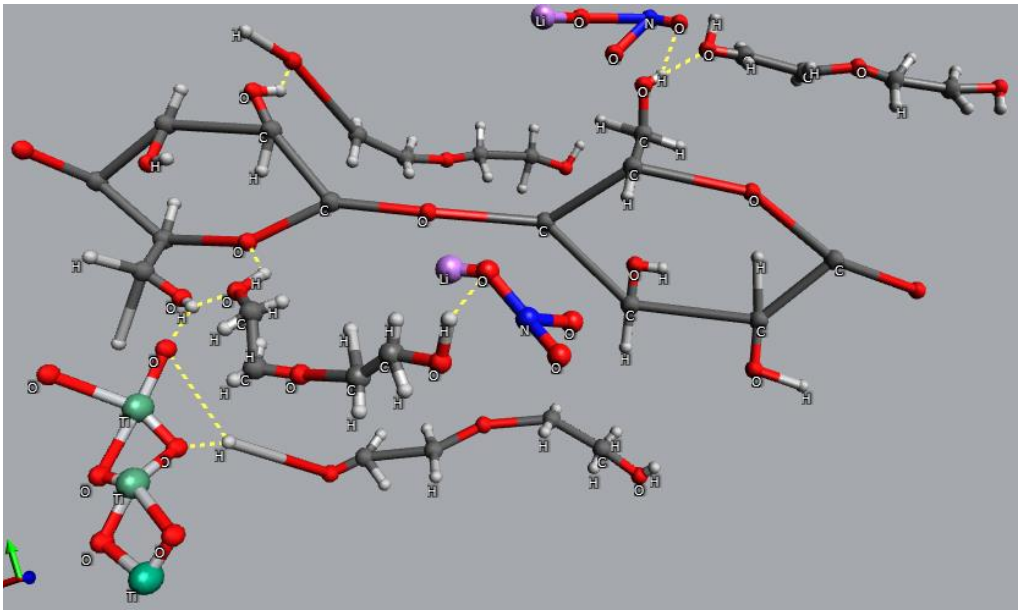

***Figure 1**. Schematic representation of polymer composite containing TiO_2 and $LiNO_3$ with hydrogen bonding*

Characterization techniques

The phase and structural properties of nano $TiO_2$and polymer blend electrolyte were investigated by Powder X-ray diffraction technique using Rigaku SmartLabSE(Japan) X-ray diffractometer with Cu-*K*α radiation, in the range 2θ from 15 to 75°, with a step size of 0.01°. The presence of functional groups, interaction of filler with polymer chains and characteristic bands corresponding to the polymer backbone were confirmed by Fourier transform infrared spectroscopy (Thermo Scientific Nicolet 6700 FT-IR Spectrometer) sweeps in the range 4000 to 400 cm^{-1}. The stability, phase transition, and decomposition of polymer blend electrolytes as a function of temperature were studied by TGA/DTA (Thermal Analysis System, Hitachi High-Tech Science Corporation, Japan). The impedance response of the polymer blend electrolytes was assessed by a Hioki IM3570 Impedance analyser, sweeping the measurement between 4 MHz to 4 Hz with a perturbation potential of 10 mV. The polymer blend electrolyte with a diameter of 1.45 cm was sandwiched between two stainless steel blocking electrodes. The temperature-dependent conductivity measurements were carried out from room temperature to 40 °C using DPI 1100 dry temperature calibrator and Hioki Impedance analyser. The linear sweep voltammetry (LSV) (between 0 and 5 V at a scan rate 10 mV s^{-1}) and chronoamperometry (polarization potential of 10 mV for 25 minutes) tests were carried out on polymer blend electrolytes by sandwiching the film in Swagelok stainless steel electrodes and recorded by OrigaFlex ($OGF^{+}500$) instrument at room temperature. The mechanical properties of polymer blend electrolytes were evaluated according to ASTM - D882 standard test by Universal Testing Machine (DAK system Inc, 7200-1KN) with a speed of 1 mm min^{-1}.

Results and discussion

Powder X-ray diffraction

The X-ray diffraction (XRD) patterns of nano TiO_2 and polymer blend electrolytes are illustrated in Figure 2. The slightly broadened XRD peaks of TiO_2 nanoparticles confirm the presence of a mixed

anatase-brookite phase. Multiple sharp diffraction peaks are observed at 2θ values of 25.35, 37.95 and 48.15°, corresponding to the (101), (103), and (200) planes of the anatase phase, respectively. These peaks closely match the JCPDS file no -00-001-0562, confirming the tetragonal phase of the TiO_2 particles within the I41/amd space group. Notably, characteristic peaks at 31.1 and 54.61° correspond to the orthorhombic brookite phase of TiO_2, attributed to the (211) and (131) planes, respectively, which is consistent with JCPDS file no- 00-002-0514. The absence of other characteristic peaks within 2θ range of 20 to 60° confirms the purity of the TiO_2 nanoparticles. These observations align with those reported by Mahata *et al.* [28]. However, the most intense peak of the brookite phase, around 54.61° is lower compared to their study and the most intense peak was observed at 27.68°.

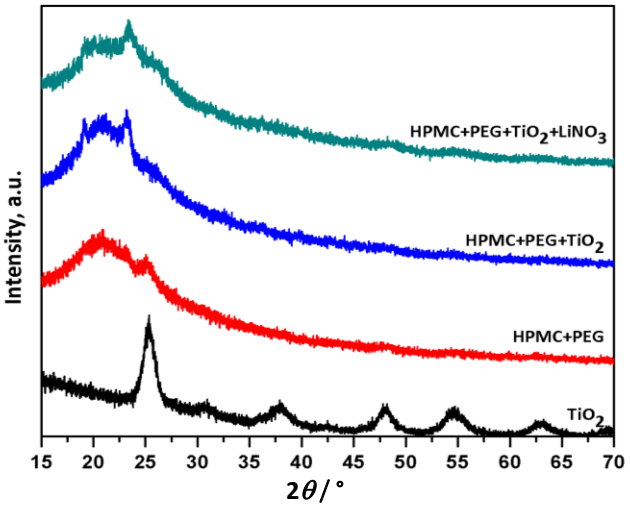

Figure 2. *X-ray diffraction patterns of TiO_2, HPMC+PEG, HPMC+PEG+TiO_2 and HPMC+PEG+TiO_2+$LiNO_3$ polymer blends*

In the mixed phases of TiO_2, the weight fraction of the brookite phase is calculated using Eq.(1) by considering the integrated intensities of both anatase and brookite phases [29]:

$$W_B = \frac{K_B I_B}{K_A I_A + K_B I_B} \quad (1)$$

where I_A and I_B are the integrated intensities of the anatase and brookite phases, respectively. The correction coefficients K_A and K_B are as mentioned elsewhere [29]. The total weight fraction of the brookite phase in the mixed phase was found to be 41.6 %. Additionally, the crystallite size of TiO_2 is determined from the obtained diffraction peaks using Debye Scherrer's equation (Eq.(2)), by considering the most intense peaks of the anatase and brookite phases separately, as mentioned elsewhere [30].

$$D = \frac{k\lambda}{\beta \cos\theta} \quad (2)$$

In Eq. (2), D, λ and β stand for crystallite size, the wavelength of Cu-$K\alpha$ radiation (0.15406 nm) and full width at half maximum of the peak, respectively.

The tetragonal phase of anatase TiO_2 has an average crystallite size of 4.94 nm with edge lengths of 0.378 and 0.956 nm, attributed a, b and c axes, respectively. Whereas the orthorhombic structure of the brookite phase has a crystallite size of 5.15 nm with edge lengths 0. 908, 0.553 and 0.518 nm along *a*, *b* and *c* axes, respectively. The characteristic c broad hump observed in XRD pattern around 20° for bare polymer blend electrolyte and polymer electrolyte containing ionic salt and nanofillers

points toward the amorphous nature of polymer electrolyte. Further, it is noteworthy that the amorphous nature of the polymer blend electrolyte is retained with the addition of TiO_2 (5 wt.%) nanofiller and $LiNO_3$ (10 wt.%) ionic salt. This confirms that added TiO_2 fillers facilitate ionic conduction paths rather than inducing crystallization in the HPMC/PEG polymer electrolyte. Moreover, a minor peak shift is observed upon the addition of nanofillers, possibly due to induced strain in the polymer blend electrolyte.

FTIR analysis

The FTIR spectra analysis enables the determination of vibrational energies associated with distinct functional groups in polymer chains and the interactions between nanofillers and polymer matrix. In this study, the FTIR spectra of the HPMC/PEG polymer blend loaded with TiO_2 and $LiNO_3$, as shown in Figure 3, were examined.

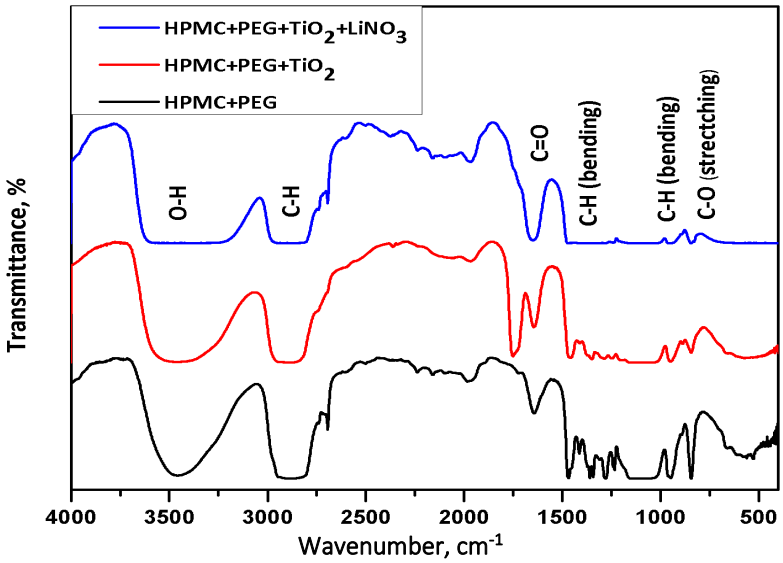

***Figure 3**. FTIR spectra of HPMC+PEG, HPMC+PEG+TiO_2 and HPMC+PEG+TiO_2+$LiNO_3$ polymer blends*

The symmetric stretching vibrations of the O-H molecule, found in both HPMC and PEG, were observed within the range of 3400 to 3600 cm^{-1}. Additionally, symmetric stretching vibrations of -CH groups in the polymer chain backbone were detected around 2880 to 2930 cm^{-1}. The band around 1450 cm^{-1} was attributed to the C-H group bending vibrations of both HPMC and PEG polymers [31]. Furthermore, stretching vibrations of C-O and C-O-C groups were identified at 1280 and 947 cm^{-1}, respectively, in HPMC polymer chains [32]. The band around 1650 cm^{-1}, indicative of carbonyl groups, was also identified by Bianchi *et al*. [33]. The presence of carbonyl groups could be attributed to the synthesis of HPMC polymer *via* esterification. Moreover, a small, negligible band at 1750 cm^{-1} in pure HPMC/PEG blends became prominent upon the addition of TiO_2, corresponding to the C=O stretching vibration due to carbonyl groups in HPMC [34]. The characteristic band corresponding to the Ti-O-Ti bending mode was observed at 569.99 cm^{-1} [35]. The introduction of nanofillers and salt into the pure HPMC/PEGpolymer blend led to noticeable shifts in these bands due to various kinds of interaction with the polymer chain. A successful fabrication of the complex HPMC/PEG/TiO_2/$LiNO_3$ polymer blend electrolyte was confirmed through the shifting and disappearance of several vibrational characteristic peaks, as summarized in Table 1.

***Table 1**. FTIR characteristic bands of polymer blend electrolytes*

Samples	Polymer blend electrolyte characteristics bands, cm^{-1}					
	O-H Stretching	C-H stretching	C=O stretching	C-H bending	C-O-C stretching	Ti-O-Ti bending
HPMC+PEG	3456.11	2896.50	1646.58	1467.58	1280, 947	--
HPMC+PEG+TiO_2	3459.03	2881.38	1646.33	1455.33	1286, 947	569.99
HPMC+PEG+TiO_2+$LiNO_3$	3406	2923.35	1650.56	1461.81	1284, 945	--

TGA/DTA analysis

The thermal transitions of the polymer electrolyte were analysed through differential thermal analysis (DTA). Figure 4a illustrates DTA thermograms of pure HPMC/PEG and HPMC/PEG/TiO_2/ $LiNO_3$ polymer blend electrolytes. The thermogram reveals that the pure HPMC/PEG polymer blend undergoes melting with an endothermic peak at approximately 60 °C. Further temperature elevation induces phase separation and subsequent polymer backbone breakage, leading to the evaporation of polymer contents. The most prominent exothermic peak around 340 °C indicates rapid vaporization of fragmented polymer molecules. The incorporation of TiO_2 and $LiNO_3$ into the polymer blend alters its properties, as evidenced by a broader melting peak, possibly due to the partial bonding of TiO_2 with the polymer chains. Additionally, the broader exothermic peak around 340 °C for polymer blend electrolyte containing filler and salt suggests slower thermal degradation of the polymer chain backbone. Thermo-gravimetric analysis (TGA) of the prepared HPMC/PEG and HPMC/PEG/TiO_2/$LiNO_3$ electrolytes was conducted within the temperature range from room temperature to 500 °C to evaluate thermal stability. The resulting TGA curve in Figure 4b indicates that the polymer blend electrolyte undergoes irreversible decomposition from 3.59 to 0.012 mg. Initial weight loss in the range of 25 to 250 °C may be attributed to the water content vaporization and polymer matrix melting. However, rapid weight loss occurs in the temperature range of 320 to 380 °C, indicating thermal stability up to 250 °C, beyond which the polymer backbone breaks down into volatile compounds.

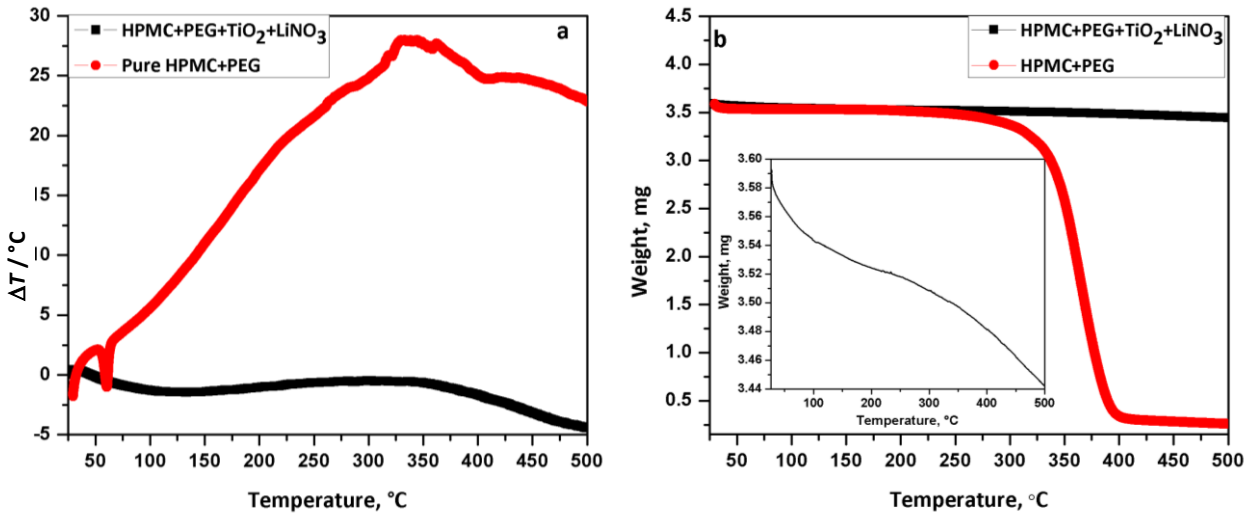

***Figure 4**. (a) DTA and (b) TGA curvesof HPMC/PEG and HPMC/PEG/TiO_2/$LiNO_3$ polymer blend electrolytes*

Above 350 °C, almost 95 % weight loss is observed as broken polymer chains and molecules completely evaporate. With the addition of TiO_2 and $LiNO_3$, the polymer becomes highly thermally stable with a weight loss of approximately 15 % at 500 °C. Furthermore, the observed initial weight loss of the composite in the range of 50 to 200 °C may be attributed to solvent and volatile molecule melting and evaporation. A slight weight loss observed in the temperature range of 200 to 280 °C

may result from strong bonds between the polymer electrolyte and nanofillers, enhancing thermal stability. Continued temperature increase leads to thermal degradation of the polymer content, consistent with existing literature [22]. However, the obtained results confirm the pronounced effect of TiO_2 and $LiNO_3$ on the thermal stability of the polymer blend electrolyte.

Impedance spectra analysis

In energy storage systems, ionic conductivity plays a pivotal role in determining their efficiency. Polymer electrolytes of higher ionic conductivity are likely to achieve optimal efficiency. An investigation of the effect of varying concentrations of TiO_2 in flexible polymer electrolyte films on the ionic conductivity was conducted through impedance spectroscopy analysis.

The Nyquist plots in Figure 5a correspond to the optimization of weight percentages of HPMC and PEG in the HPMC/PEG polymer blend electrolyte. For all polymer blends, semicircle responses at higher to mid-frequency ranges and some spikes at the lowest frequencies suggest a dominance of the bulk polymer blend electrolyte impedance over interfacial electrolyte/electrode response.

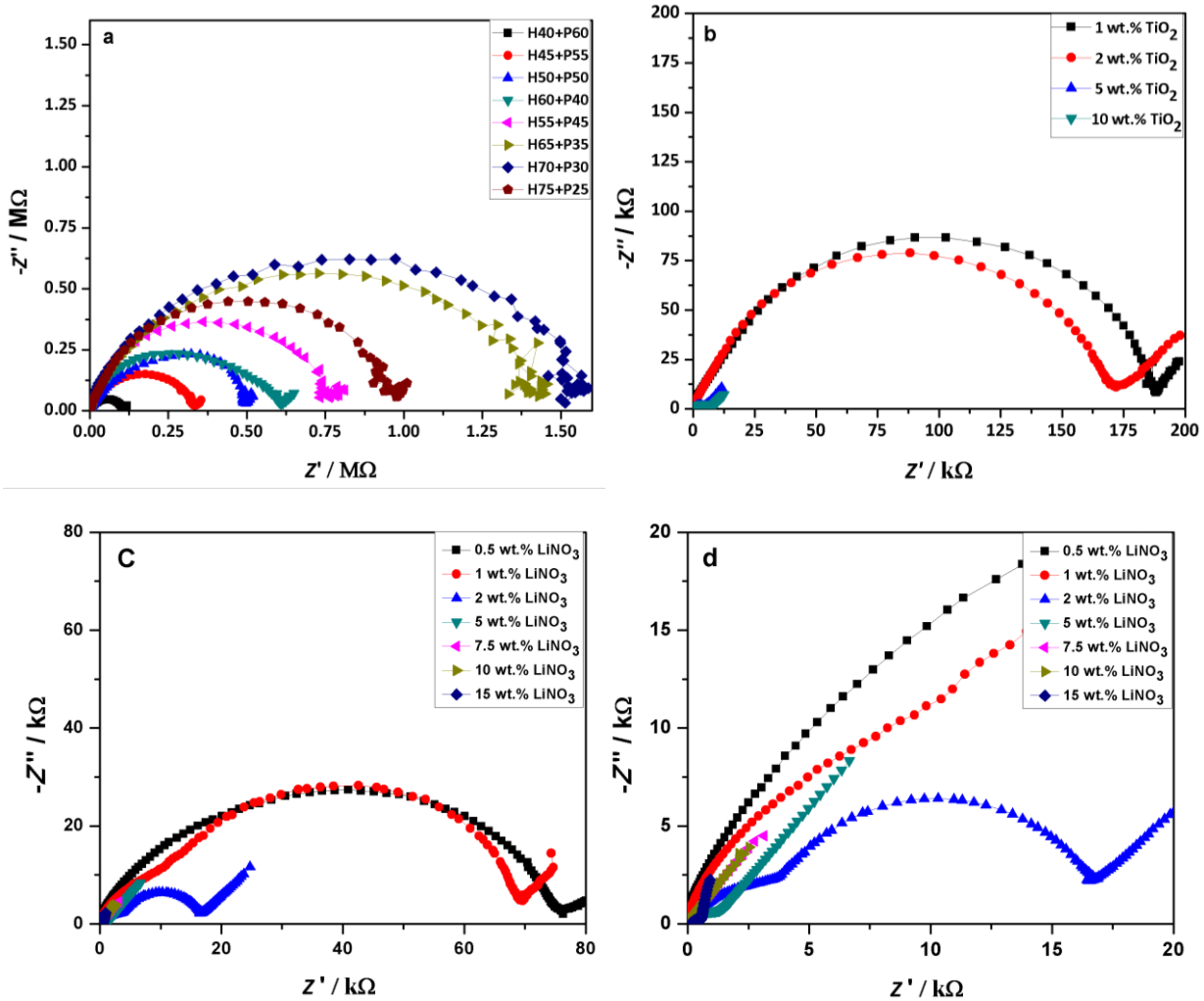

***Figure 5**. Nyquist plots of (a) HPMC/PEG, (b) HPMC/PEG/TiO_2, (c) HPMC/PEG/TiO_2/$LiNO_3$, (d) enlarged view of HPMC/PEG/TiO_2/$LiNO_3$ at higher frequencies*

Semicircle diameters are determined by the bulk ionic resistance (R_b) values, which are relatively high, from about 1.5 MΩ for the HPMC(70)/PEG (30) polymer blend electrolyte. The notable reduction in semicircle diameters down to about 0.125 MΩ was observed with increasing PEG concentration within the HPMC polymer matrix up to 60 wt.%. This reduction may be due to improved chain mobility

at optimized weight percentages, where PEG acts as a plasticizer [36]. Additionally, blending polymers induced controlled phase separation, creating additional grain boundaries conducive to ion mobility within the host polymer matrix [37]. It was observed that the HPMC(40)/PEG(60) showed the lowest R_b value. At the same time, it has lower mechanical strength and is highly brittle, with noticeable phase separation. In contrast, the HPMC(45)/PEG(55) blend exhibited better mechanical strength and flexibility. Therefore, HPMC(45)/PEG(55) was chosen as the optimized pure polymer blend electrolyte. Additionally, TiO_2 was added as a nanofiller to the HPMC(45)/PEG(55) blend.

The Nyquist plots for HPMC(45)/PEG(55-y)/TiO_2(y),(y = 1, 2, 5 and 10 wt.%) polymer blend electrolytes at room temperature are shown in Figure 5b. These impedance plots exhibit depressed semicircles due to the bulk ionic resistance of polymer electrolytes, followed by Warburg impedance, seen as a -45° slope line in the lower frequency region. The appearance of Warburg impedance indicates the presence of ionic diffusion in the electrolyte toward blocking electrodes [38]**.** The decreasing trend of R_b with the addition of TiO_2 fillers from about 0.2 MΩ at 1 wt.% TiO_2, to less than 10 kΩ at 5 wt.% TiO_2 (Figure 5b) is attributed to improved chain mobility. However, further increase in TiO_2 above 5 wt.% exhibited a contrary effect on R_b. Additionally, the presence of a slope line in the low-frequency range of the Nyquist plot indicates ion diffusion through grain boundaries formed by the composite [38]. Hence 5 wt.% TiO_2 loaded HPMC/PEG was chosen as an optimized polymer blend electrolyte.

Finally, lithium nitrate ($LiNO_3$) ionic salt was incorporated into the optimized HPMC/PEG/ /TiO_2 polymer blend electrolyte in varying weight percentages, ranging from 0.5 to 15 wt.%, as illustrated in Figures 5c and 5d and outlined in Table 2. Observations revealed that at 0.5 and 1 wt.% of $LiNO_3$, R_b value remained high, at about 77.4 and 67.6 kΩ, respectively. At 2 wt.% of $LiNO_3$, R_b values decreased, while impedance spectra comprised two semicircles (Figure 5c). The diameter of the first semicircle can be ascribed to R_b while the other, to a contribution of impedance attributed to the electrode-electrolyte interface, where some interfacial charge transfer resistance is followed by Warburg diffusion impedance. As $LiNO_3$ concentration further increased up to 10 wt.%, both R_b and charge transfer resistances decreased, leading to a noticeable reduction in the diameters of both semicircles (Figure 5d). This reduction, resulting from the increased number of ionic charges generated by added $LiNO_3$ ionic salt, indicates a dominance of ionic diffusion and implies that most ions are effective charge carriers [39]. Upon further increasing of $LiNO_3$ concentration above 10 wt.%, a semicircle re-appeared in the mid-frequency region, possibly due to alterations in the polymer electrolyte owing to ionic agglomeration, ionic collision and hence the formation of double layer capacitance, which results in the increase of charge transfer resistance [40].

Optimization of polymer blend composite electrolyte through ionic conductivity evaluation

The ionic conductivity (σ) of the polymer blend electrolytes was calculated using Eq. (3)

$$\sigma = \frac{d}{R_b A} \tag{3}$$

where d and A represent the thickness and area of the polymer electrolyte, respectively. The bulk resistance R_b values were measured from Nyquist plots as intercepts on the Z'-axis.

For the HPMC/PEG/TiO_2 polymer electrolyte of thickness in the range of 60-85 μm, an increase of TiO_2 concentration up to 5 wt.% resulted in an enhancement of the ionic conductivity of films that was found to increase from 0.0283 μS cm^{-1} (at 1 wt.% TiO_2) to 1.02 μS cm^{-1} (at 5 wt.% of TiO_2). This increase can be attributed to the formation of more mobile chains within the polymer electrolyte. Additionally, the Lewis acid-base inherent characteristics exhibited by TiO_2 and polymer chains could increase the amorphous phase of polymer blend electrolyte, providing a potential tunnel for ion migration [12].

Further increase of TiO_2 content reduces ionic conductivity to 0.624 μS cm^{-1}. The reduction of ionic conductivity is possibly due to aggregation of nanofillers impeding ionic conductivity by blocking interfacial pathways along with reduced salt disassociation and chain mobility [22]. Hence, 5 wt.%TiO_2 would be the optimal concentration in HPMC/PEG/TiO_2 polymer blend electrolyte that shows better performance. Following the optimization of the TiO_2, we incorporated the ionic salt $LiNO_3$ by adjusting the weight percentages of PEG and HPMC, as outlined in Table 2.

***Table 2**. Optimization of HPMC/PEG/TiO_2/$LiNO_3$ polymer blend electrolyte*

Sample code	Polymer blend content, wt.%				R_b / Ω	σ / μS cm^{-1}
	HPMC	PEG	TiO_2	$LiNO_3$		
HPTL 1	45	49.5	5	0.5	77400	0.921
HPTL 2	45	49.0	5	1	67600	1.65
HPTL 3	45	48.0	5	2	8360	5.25
HPTL 4	42.5	47.5	5	5	455	12.5
HPTL 5	42.5	45.0	5	7.5	69.02	80.5
HPTL 6	42.5	42.5	5	10	38.2	213
HPTL 7	40.0	40.0	5	15	611	6.47

As the concentration of $LiNO_3$increased from 0.5 to 10 wt.%, the ionic conductivity of the electrolyte films (with thicknesses ranging from 120 to 150 μm) improved significantly, ranging from 0.921 μS cm^{-1} to 0.213 mS cm^{-1}. This observation suggests that the addition of Li salts increases the concentration of ions serving as charge carriers within the polymer matrix, thereby enhancing ionic conductivity. Meanwhile, TiO_2 facilitates ion migration by reducing the crystallinity of the polymer [41]. Furthermore, the polymer blend electrolyte acts as a solid solvent containing hydroxyl (-OH) groups, where oxygen is partially negative, and hydrogen is partially positive. The partially positive hydrogen ions interact and form hydrogen bonds with the negatively charged NO_3^- ions of $LiNO_3$, promoting the dissociation of $LiNO_3$ salt and facilitating the release of more Li^+ ions. Nevertheless, the electrostatic attraction between Li^+ and NO_3^- ions may be diminished as a result of hydrogen bond formation. Additionally, the surface charge of TiO_2 competes with Li ions in forming complexes with polymer chains, thereby altering the structure and promoting the creation of more ionic conduction pathways [42]. This behaviour was also observed by Sasikumar *et al*. [22] in their study. It is worth mentioning that the polymer composite with 15 wt.% of $LiNO_3$ exhibits high hygroscopicity and adhesive surface in nature, while the ionic conductivity of the film reduces to 6.47 μS cm^{-1} (Table 2). Table 3 summarizes optimization results based on ionic conductivity obtained for HPMC/PEG, HPMC/PEG/TiO_2 and HPMC/PEG/TiO_2/$LiNO_3$ polymer blend electrolytes.

***Table 3.** Estimated bulk resistance and ionic conductivity for optimized wt.% of polymer blend electrolytes*

Sample	Optimized polymer blend electrolyte content, wt.%				Bulk resistance, Ω	σ / μS cm^{-1}
	HPMC	PEG	TiO_2	$LiNO_3$		
HPMC/PEG	45	55	0	0	2.87×10^5	0.02
HPMC/PEG/TiO_2	45	50	5	0	3.99×10^3	1.02
HPMC/PEG/TiO_2/$LiNO_3$	42.5	42.5	5	10	38.2	213

Jonscher's power law

The relationship between AC conductivity and the types of involved charge carriers, including electrons, ions and defects, can be related by Jonscher power law given by Eq. (4)

$$\sigma_{AC} = \sigma_{DC} + A\omega^2 \quad (4)$$

where ω is the hopping frequency, *A* is the pre-exponential factor, and *s* denotes the interaction of charge carriers during the hopping process. Also, both AC and DC conductivities are related by the type of charge carriers involved in conduction. Eq. (4) was used to fit the alternating current conductivity (σ_{ac} / S cm^{-1}) as a function of the logarithm of frequency (log ω), as demonstrated for the optimized HPMC/PEG, HPMC/PEG/TiO_2, and HPMC/PEG/TiO_2/$LiNO_3$ polymer blend electrolytes in Figure 6(a-c). Table 4 summarizes the estimated parameter values from the Jonscher power law fitting.

In the case of the pure HPMC/PEG blend (Figure 6a, Table 4), the AC conductivity remains relatively constant in the lower and mid-frequency range but exhibits an increase at higher frequencies.

***Table 4**. Estimated parameter values from Jonscher power law fitting (for optimized conditions)*

Sample code	σ_{DC} / µS cm^{-1}	*A*	*s*
(HPMC+PEG)	0.016	1.99×10^{-10}	0.58
(HPMC+PEG+TiO_2)	0.08	9.93×10^{-9}	0.36
(HPMC+PEG+TiO_2+$LiNO_3$)	1.38	3.85×10^{-8}	0.84

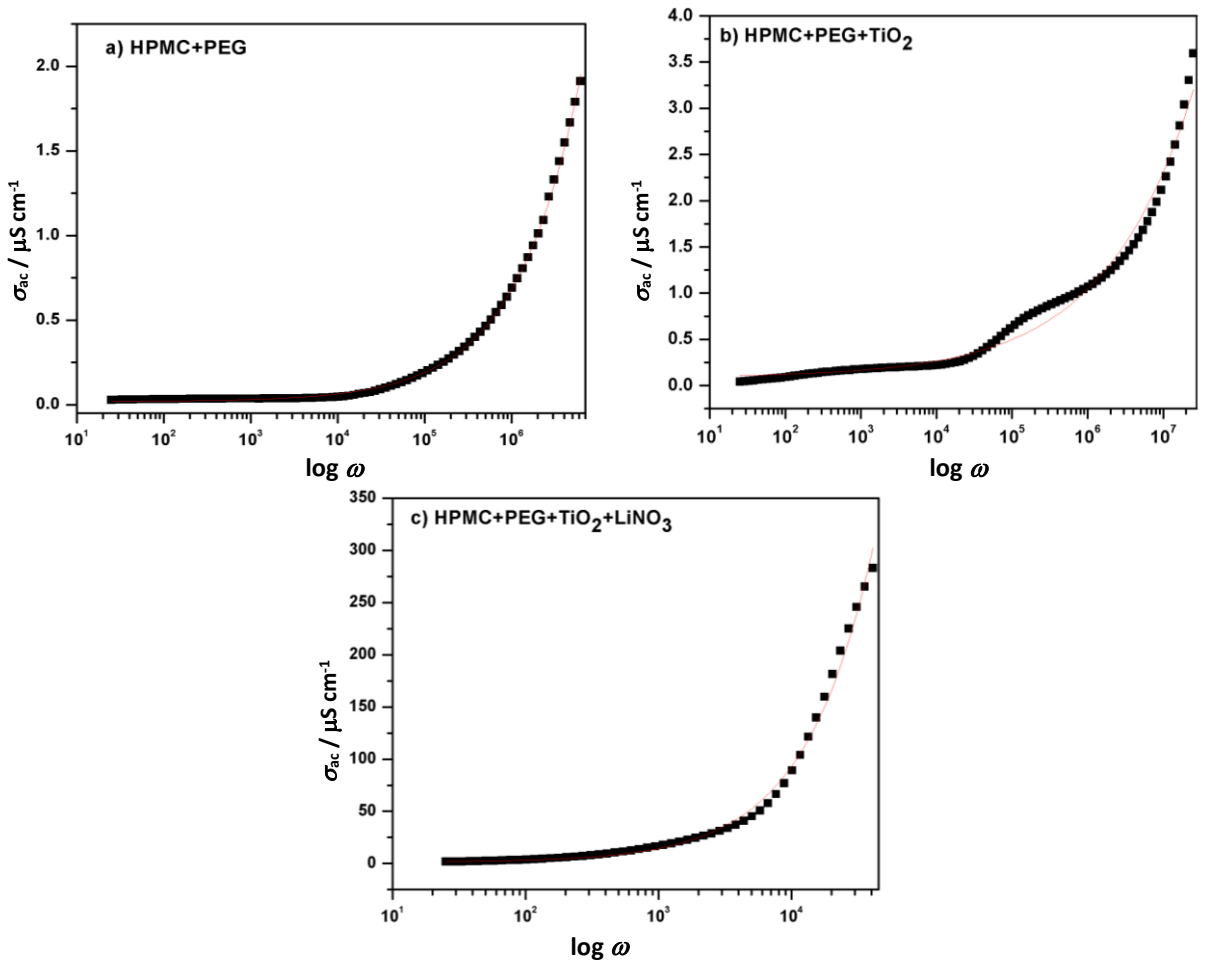

***Figure 6**. Jonscher power law fitting for (a) HPMC/PEG, (b) HPMC/PEG/TiO_2, and (c) HPMC/PEG/TiO_2/$LiNO_3$ polymer blend electrolytes*

The increased conductivity at higher frequencies is due to two main factors: firstly, to the protonation and deprotonation of polar functional groups (such as -OH and -O- groups) along with enhanced segmental motion, and secondly, the hopping of ions between sites, a phenomenon observed in the Grotthuss mechanism [43]. However, the pre-factor *A*, which corresponds to the frequency-dependent conductivity, is found to be 1.99×10^{-10}, two orders of magnitude lower than

DC conductivity. This suggests that the DC conductivity predominates. The parameter *s* is 0.58, which is less than 1, indicating multiple ion relaxation processes [38].

Upon introduction of TiO_2 into the polymer electrolyte (Figure 6b, Table 4), the pre-factor *A* increases by an order of magnitude while the value of *s* decreases. This indicates either a slightly slower backward motion of the charge carriers with respect to frequency or a change in the site relaxation time. Nevertheless, the DC conductivity increases, but the order of magnitude of DC conductivity remains the same [38]. With the addition of $LiNO_3$ (Figure 6c, Table 4), the AC conductivity starts to increase in the mid-frequency range. The DC conductivity experiences a substantial enhancement, reaching 1.38 μS cm^{-1}, representing a two-order-of-magnitude increase. The pre-factor *A* also increased to 3.85×10^{-8}, suggesting the frequency-dependent relationship of conductivity. Additionally, the parameter *s* attains a value of 0.844, approaching unity, which signifies a pronounced dependence of AC conductivity on frequency. At higher frequencies, the increase in conductivity corresponds to enhanced mobility of Li ions within the polymer matrix. Furthermore, the Jonscher power law fitting confirms that the increased conductivity is indeed a consequence of a greater number of ions present [38].

Effect of aging on the optimized HPMC/PEG/TiO_2/$LiNO_3$ polymer blend electrolyte

Impedance analysis was conducted to observe the behaviour of the optimized HPMC/PEG/ /TiO_2/$LiNO_3$ polymer blend electrolyte over time (1 to 6 days) (Figure 7). The results suggested that the resistance of the optimized polymer blend electrolyte containing 10 wt.% of $LiNO_3$ salt was mainly determined by the interfacial resistance. Figure 7 illustrates that the polymer blend electrolyte experienced notable changes in resistance with aging. Initially, on day 1, the interfacial resistance at the low-frequency intercept in Figure 7 was 84.8 Ω. By day 3, this resistance decreased to 38.2 Ω and then increased significantly to 82.0 Ω by day 5, after which it stabilized. These results suggest that the polymer electrolytes could exhibit improved interfacial stability after an optimal storage period, thereby enhancing performance. The reduction in resistance may be attributed to moisture absorption, possibly facilitated by the ability of nano TiO_2 to effectively retain the solvent through capillary action, allowing the polymer chain to undergo a relaxation process and creating more flexible pathways for ions [42].

Saikumar *et al.* [22] reported that TiO_2-doped HSPE polymer composite film undergoes a significant variation in interfacial resistance, which rises from 154 to 758 Ω and reduces and stabilizes at 490 Ω after 10 days and claims that TiO_2-HSPE has better interfacial stability. A study by Zhai *et al.* [42] on polymer composite made of TiO_2 and PVDF-HFP in addition to the ionic liquid reported that interfacial resistance of the sample NCPE-0 increased from 250 to 850 Ω after 12 days and reached a steady value of 900 Ω, whereas their sample NCPE-2 reaches a steady value of 400 Ω after 8 days.

The temperature-dependent Nyquist plots of optimized HPMC/PEG/TiO_2/$LiNO_3$ polymer blend electrolyte as a function of temperature are shown in Figure 8. The temperature-dependent ionic conductivity studies were carried out on the optimized polymer blend electrolyte on day 7 (after stabilization).

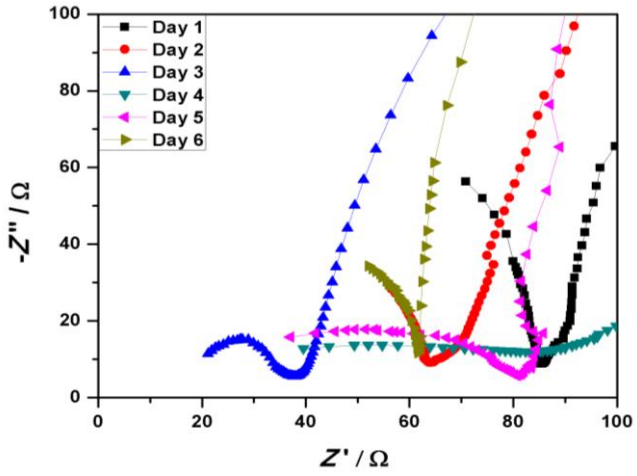

***Figure 7**. Nyquist plots of optimized HPMC+PEG+TiO_2+$LiNO_3$ polymer blend electrolyte aged up to 6 days*

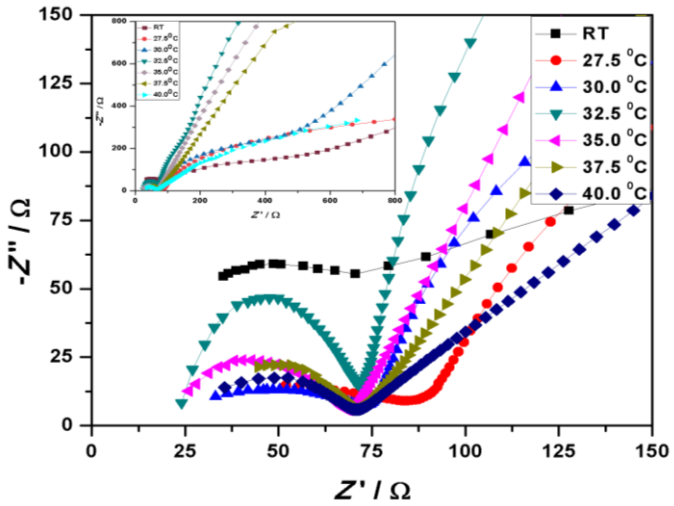

***Figure 8**. Temperature-dependent Nyquist plots of optimized HPMC/PEG/TiO_2/$LiNO_3$ polymer blend electrolyte*

The ionic conductivity increases from 0.099 to 0.119 mS cm^{-1} as temperature rises from room temperature (26 °C) to 40 °C. The Nyquist plots at room temperature, 27.5 and 30 °C have two semicircles. The mid-frequency semicircle indicated charge transfer resistance likely due to ionic agglomeration, while the high-frequency semicircle corresponds to the bulk of the solid electrolyte (on day 7) [6]. Interestingly, above 35 °C, the slope line corresponding to ionic diffusion dominates, while the interfacial resistance of the polymer electrolyte is also reduced. This confirmed that distributed nano TiO_2 in the polymer matrix will enhance the conductivity by creating voids and defects in the polymer matrix, thus preventing the crystallization of the polymer matrix. In addition, the polymer blend undergoes a thermal expansion above 30 °C, improving the motion of polymer chains and favouring the mobility of ionic charge carriers [42]. However, no significant improvement in ionic conductivity was observed above 37.5 °C.

The Arrhenius equation (5) corresponds to the temperature-dependent hopping mechanism of ions in polymer blend electrolytes. The Arrhenius plot of ln σ *vs*. 1000 T^{-1} for optimized polymer blend electrolytes follows a linear relationship as depicted in Figure 9, confirming the Arrhenius behaviour. The plot reveals that optimized quantities show stronger temperature dependence.

$$\sigma = \sigma_0 e^{\frac{-E_a}{kT}} \quad (5)$$

In Eq. (5), $\sigma_0$is the pre-exponential factor, E_a is the activation energy, k is the Boltzmann constant and T is the absolute temperature. By linear fitting the above equation, the estimated value of activation energy E_a is 0.1 eV. Quite close comparable values were reported by Trevisanello *et al*. [40] for Li|PEO, LLZO|PEO and lithium aluminium titanium phosphate (LATP)|PEO electrolytes. The work of Wang *et al*. [44] on pure lithium aluminium germanium phosphate (LAGP) and PEO/LAGP/LiTFSI composite materials reported an activation energy of 0.32 and 0.99 eV, respectively. Additionally, they reported that ice-templated LAGP/PEO attains 1.11 mS cm^{-1} at 60 °C and corresponding activation energy of 0.45 eV. Similarly, Ahmed *et al*. [45] reported that 70 % of $LiSn_2(PO_4)_3$ (LSP powder) in PEO/$LiClO_4$ composite has an activation energy of 0.34 eV in the temperature range 27 to 60 °C which is impressively less than pure LSP powder whereas the conductivity is maximum of 0.118 mS cm^{-1} at 60 °C. Zhai *et al.* [42] reported that activation energy in PVDF-HFP polymer composite containing TiO_2 and ionic liquid decreases with an increase in TiO_2 concentration. Mei *et al.* [46] reported the activation energy as high as 1.67 to 1.77 eV for LLZTO added PEO-based polymer composite material. They also noted that the crystalline phase of the polymer electrolyte necessitates higher activation energy due to the increased energy required for ion migration compared to the amorphous phase.

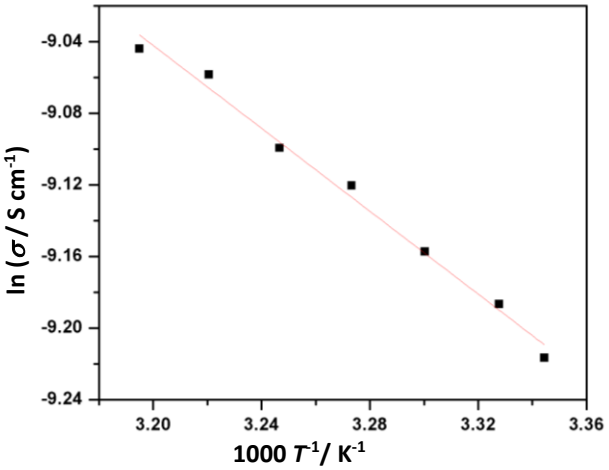

***Figure 9**. Arrhenius plot of ln σ* vs. *1000* T^{-1} *of optimized HPMC/PEG/TiO_2/$LiNO_3$ polymer blend electrolyte*

The total conductivity of the composite is influenced by both cation and anion movement, as well as electronic conduction. The transference number of cations within an electrolyte significantly impacts recyclability and overall battery performance. Cation transport can be estimated using the Bruce-Vincent equation (6):

$$t_+ = \frac{I_{SS}\left(\Delta V - I_0 R_0\right)}{I_0\left(\Delta V - I_{SS} R_{SS}\right)} \tag{6}$$

where I_0, I_{SS}, R_0 and R_{SS} represent the initial current, steady-state saturation current, and interfacial resistance before and after polarization, respectively. The initial and steady-state currents were determined using potentiostatic polarization, where current is measured over time at the constant potential of 10 mV, with the polymer electrolyte sandwiched between two non-blocking stainless steel electrodes. The potentiostatic polarization curve at 10 mV DC bias for 1500 seconds and Nyquist plots before and after polarization are depicted in Figure 10a and b, respectively.

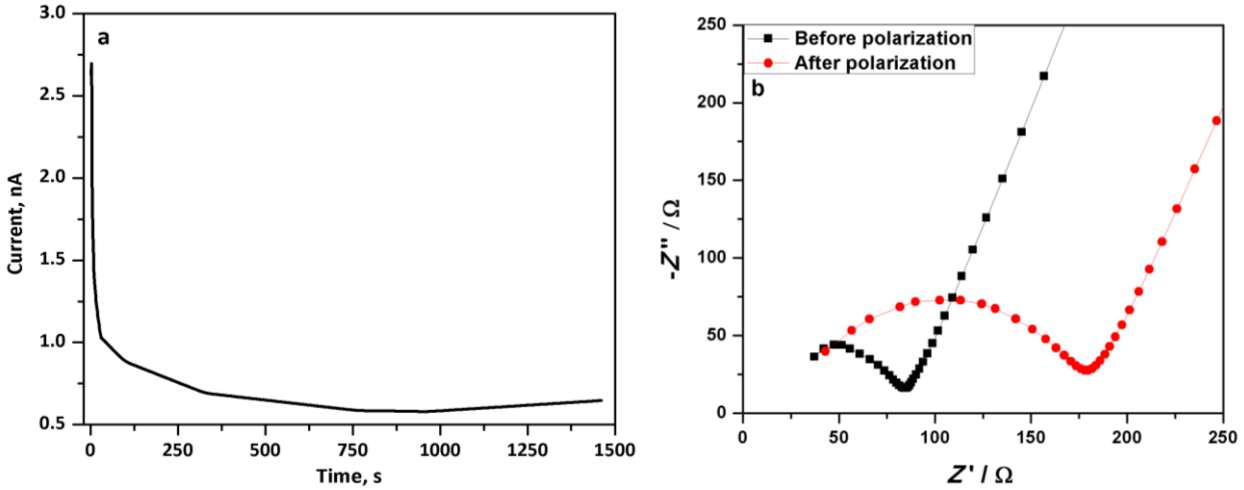

Figure 10.*(a) Chronoamperometry response of optimized HPMC/PEG/TiO_2/$LiNO_3$ polymer blend composite electrolyte at 10mV bias, (b) Nyquist plots before and after polarization*

Initially, the polarization current of 2.61 nA decreases over time, reaching a steady value of 0.58 nA after 650 s. The initial maximum current indicates the movement of all ionic species within the host polymer matrix, suggesting the contribution of both Li cations and nitrate anions as charge carriers, resulting in higher currents. The current exponentially decreases with time, reaching a steady state where only cationic species are involved in conductivity. The Nyquist plot after potentiostatic polarization shows higher interfacial resistance, indicating the formation of an anionic layer at the interface that may impede cation movement. Calculations reveal that the highest transference number for the optimized polymer blend composition is 0.323, a considerable value for battery fabrication, closely resembling polymer electrolytes with liquid plasticizers [47]. Previous study by Deivanayagam *et al*. [47] reported a transference number (t_+) value of 0.23 for highly cyclable polymer electrolytes for Mg batteries. Hu *et al.* [48] reported Li-ion transference numbers of 0.51 and 0.3 for Li/Al-SE/Li and Li/SE/Li cells, respectively, with enhanced ionic conductivity and dendrite suppression through the incorporation of alumina.

A new strategy for Li-based batteries with increased energy density, a wide electrochemical window, and excellent ionic conductivity has gained tremendous interest. To ensure the safety and cycling performance of batteries, an electrolyte with higher electrochemical and thermal stability is preferred. To assess the electrochemical potential window of the polymer electrolyte, linear sweep voltammetry (LSV) was conducted by sandwiching the polymer electrolyte between stainless-steel electrodes, with a scan rate of 1.0 mV s^{-1} at room temperature across the range of 0 to 5V as depicted in Figure 11.

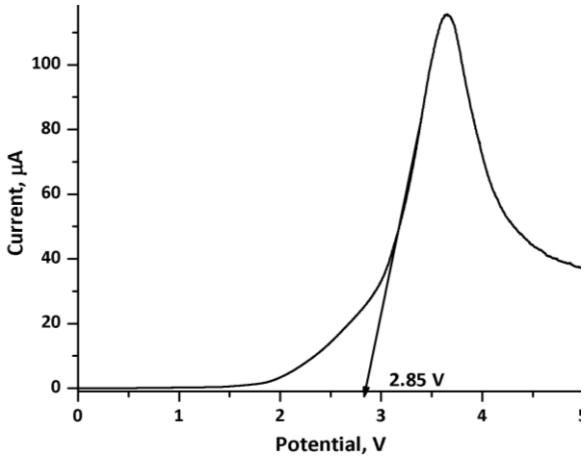

Figure 11. *Linear sweep voltammogram of optimized HPMC/PEG/TiO_2/$LiNO_3$ polymer blend electrolyte*

The observed increase in anodic current with potential corresponds to the degradation and decomposition of the polymer matrix and, hence, the contribution from anions present in the matrix [22,49]. However, an anodic peak is observed at 3.5 V, indicating an oxidation reaction of the polymer. The results show that the optimized polymer electrolyte has a relatively narrow chemical stability window of 2.85 V, determined by the intercept of the rapid current change curve on the voltage axis at zero current. These findings highlight the safe use of optimized polymer electrolytes in batteries with low-voltage cathode materials, ideally operating below 2.8 V.

Mechanical properties of optimized polymer blend electrolytes

Ensuring the safety and reliability of polymer electrolytes is crucial in Li-ion batteries. The strong mechanical integrity of solid-state electrolytes in batteries directly correlates with safety and reliability. The mechanical reliability is based on tensile strength, owing to the subsidiary properties in comparison with Ionic conductivity and growth of Li dendrite through polymer films. While the ionic conductivity of polymer films improves with enhanced flexibility, introducing organic plasticizers can compromise the mechanical integrity of these films. Consequently, achieving a balance between flexibility and mechanical strength becomes imperative to suppress dendrite growth effectively. Strategies such as incorporating nanofillers and reinforcement agents improve mechanical strength and suppress dendrite proliferation. A polymer electrolyte with good flexibility and mechanical strength is desired for the practical implementation in batteries [50].

The mechanical properties were evaluated using stress *vs.* strain curve for HPMC/PEG, HMC/ /PEG/TiO_2andHPMC/PEG/TiO_2/$LiNO_3$ polymer blend electrolytes, as demonstrated in Figure 12. Evaluated mechanical properties of optimized HPMC/PEG, HPMC/PEG/TiO_2 and HPMC/PEG/TiO_2/ /$LiNO_3$ polymer blend electrolytes are summarized in Table 5.

Table 5. *Mechanical properties of optimized polymer blend electrolytes*

Sample	Tensile strength, MPa	Elongation at break, %
HPMC/PEG	0.470	0.493
HPMC/PEG/TiO_2	2.838	1.866
HPMC/PEG/TiO_2/$LiNO_3$	5.700	6.021

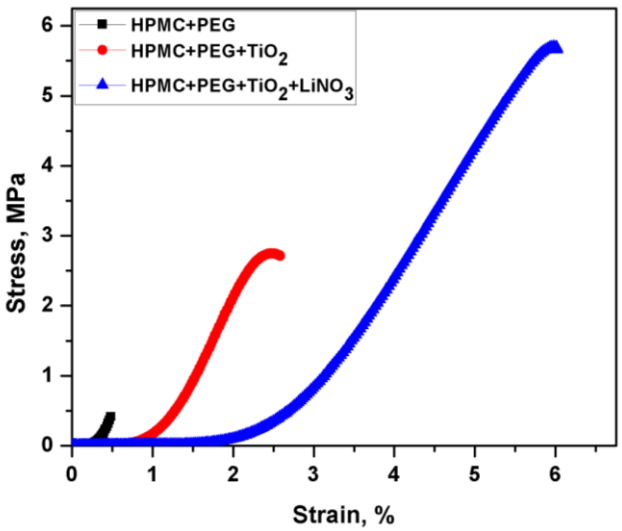

Figure 12*. Tensile strength of optimized HPMC/PEG, HPMC/PEG/TiO_2 and HPMC/PEG/TiO_2/$LiNO_3$polymer blend electrolytes*

Pure polymer blend HPMC/PEG exhibits a tensile strength of 0.470 MPa, whereas the introduction of 5 wt.% TiO_2 yields a notable increase to 2.83 MPa. Further tensile strength increased to 5.7 MPa by incorporating 10 wt.% $LiNO_3$. This improvement in tensile strength can be attributed to the interaction between nanofillers and polymer chains, imparting a reinforcing effect. The enhanced mechanical strength of polymer electrolytes is due to the uniform dispersion of nanofillers and the strong adhesion effect between nanofiller and polymer matrix. However, the introduction of inorganic filler into the polymer matrix may reduce flexibility due to the creation of defects and voids. Sasikumar *et al.* [22] reported the maximum mechanical strength of 9.3 MPa for 10 wt.% of TiO_2-NCF polymer electrolyte with ionic conductivity in the range of mS cm^{-1}. Song *et al.* [51] studied a gel polymer electrolyte for Li-ion batteries and reported a maximum mechanical strength of 4.07 MPa with good ionic conductivity of 6.22 mS cm^{-1}. It can be stated at the end that the optimized HPMC/PEG/TiO_2/ /$LiNO_3$ polymer electrolyte contains 5 wt.% TiO_2 with 10 wt.% $LiNO_3$ exhibits both good ionic conductivity and mechanical strength, making it a promising material for battery fabrication.

Conclusion

A flexible HPMC/PEG/TiO_2/$LiNO_3$ polymer blend electrolytes were fabricated by the solution casting method. XRD analysis confirmed that the addition of nano TiO_2 has no effect on the amorphous nature of the polymer film. FTIR analysis confirms the functional groups and their interactions within the polymer electrolyte. The observed shifts in the FTIR spectra bands are due to the interactions between TiO_2, the polymer chains, and $LiNO_3$. The thermal stability and phase transition of the flexible polymer blend electrolyte were evaluated by TGA/DTA analysis and found that enhanced thermal stability around 340 °C and a broader melting point. Nyquist plots indicated that the optimized HPMC/PEG/TiO_2/$LiNO_3$ (5 wt.% TiO_2 and 10 wt.% $LiNO_3$) polymer blend electrolyte exhibited a maximum ionic conductivity of 0.213 mS cm^{-1} at room temperature. This enhanced conductivity suggests that the nanofillers facilitate additional pathways for ion migration. The temperature-dependent ionic conductivity followed linear Arrhenius behaviour, with a fitted activation energy of 0.1 eV. Jonscher power law fitting showed that the pure HPMC/PEG blend primarily contributed to DC conductivity, while the HPMC/PEG/TiO_2/$LiNO_3$ polymer blend electrolyte had a higher contribution from the frequency-dependent parameter A and s of the Arrhenius equation. The optimized polymer blend electrolyte, placed between stainless steel electrodes and polarized at 10 mV for 25 minutes, achieved a maximum Li ion transference number of 0.323. Linear sweep voltammetry, conducted at a scan rate of 1.0 mV s^{-1} up to 5 V, revealed an electrochemical stability window of 2.85 V, with an oxidation peak at 3.5 V. The tensile strength of the polymer blend electrolytes improved with the addition of the nanofiller due to its reinforcing effect, reaching 5.70 MPa for the optimized polymer blend. Future research work will be focused on optimizing the composition through software-assisted experimental designs, incorporating ionic liquid, co-fillers, and introducing microporous structural defects.

Authorship contribution statement: *Mohan S: Conceptualization, Methodology, Investigation, Data acquisition and analysis, visualization, original draft writing and editing. Rajashekar F Bhajantri: Conceptualization, Project administration, Supervision, Funding acquisition, formal analysis, review and editing.*

Declaration of competing interests: *Authors declare no competing financial or personal relationships that could influence the work reported in this project.*

Submission declaration: *The authors declare that the manuscript is our original work and all the authors contributed significantly. Further, this work is not previously published and not under consideration elsewhere.*

Funding agency: *Science and Engineering Research Board (SERB), Department of Science and Technology (DST), Ministry of Science and Technology, Government of India (File No. EEQ/2022/001028).*

Acknowledgements: *The authors acknowledge the Science and Engineering Research Board, Department of Science and Technology, Government of India, New Delhi for the Research Project (EEQ/2022/001028). Also, the authors are thankful to SAIF, Karnatak University Dharwad for XRD& FTIR Facilities. Authors acknowledges support from Dr. Saraswati Masti and her students, Department of Chemistry, Karnataka Science College, Dharwad for providing Universal Testing Machine facility.*

References

[1] T. Juqu, S. C. Willenberg, K. Pokpas, N. Ross, Advances in paper-based battery research for biodegradable energy storage, *Advanced Sensor and Energy Materials* **1** (2022) 100037. https://doi.org/10.1016/j.asems.2022.100037

[2] L. Yang, X. Kong, F. Li, H. Hao, Z. Cheng, H. Liu, J.-F. Li, S. Zhang, Perovskite lead-free dielectrics for energy storage applications, *Progress in Materials Science* **102** (2019) 72-108. https://doi.org/10.1016/j.pmatsci.2018.12.005

[3] E. E. R. Gómez, J. H. M. Hernandez, Obtaining Electrospun Membranes of Chitosan/PVA and TiO_2 as a Solid Polymer Electrolyte with Potential Application in Ion Exchange Membranes, *Membranes* **13** (2023) 862. https://doi.org/10.3390/membranes13110862

[4] R. Borah, F. R. Hughson, J. Johnston, T. Nann, On battery materials and methods, *Materials Today Advances* **6** (2020) 100046. https://doi.org/10.1016/j.mtadv.2019.100046

[5] N. Takami, M. Sekino, T. Ohsaki, M. Kanda, M. Yamamoto, New thin lithium-ion batteries using a liquid electrolyte with thermal stability, *Journal of Power Sources* **97**-**98** (2001) 677-680. https://doi.org/10.1016/S0378-7753(01)00699-1

[6] J. Chattopadhyay, T. S. Pathak, D. M. F. Santos, Applications of Polymer Electrolytes in Lithium-Ion Batteries, *Polymers* **15** (2023) 3907. https://doi.org/10.3390/polym15193907

[7] W. Ren, C. Ding, X. Fu, Y. Huang, Advanced gel polymer electrolytes for safe and durable lithium metal batteries: Challenges, strategies, and perspectives, *Energy Storage Materials* **34** (2021) 515-535. https://doi.org/10.1016/j.ensm.2020.10.018

[8] J. Castillo, A. Santiago, X. Judez, I. Garbayo, J.A. Coca Clemente, M.C. Morant-Miñana, A. Villaverde, J. A. González-Marcos, H. Zhang, M. Armand, C. Li, Safe, Flexible, and High-Performing Gel-Polymer Electrolyte for Rechargeable Lithium Metal Batteries, *Chemistry of Materials* **33** (2021) 8812-8821. https://doi.org/10.1021/acs.chemmater.1c02952

[9] S. Das, A. Ghosh, Symmetric electric double-layer capacitor containing imidazolium ionic liquid-based solid polymer electrolyte: Effect of TiO_2 and ZnO nanoparticles on electrochemical behavior, *Journal of Applied Polymer Science* **137** (2020) 48757. https://doi.org/10.1002/app.48757

[10] X. Pan, P. Yang, Y. Guo, K. Zhao, B. Xi, F. Lin, S. Xiong, Electrochemical and Nanomechanical Properties of TiO_2 Ceramic Filler Li-Ion Composite Gel Polymer Electrolytes for Li Metal Batteries, *Advanced Materials Interfaces* **8** (2021) 2100669. https://doi.org/10.1002/admi.202100669

[11] A. A. Al-Muntaser, R. A. Pashameah, A. E. Tarabiah, E. Alzahrani, S. A. AlSubhi, A. Saeed, A. M. Al-Harthi, R. Alwafi, M. A. Morsi, Structural, morphological, optical, electrical and dielectric features based on nanoceramic $Li_4Ti_5O_{12}$ filler reinforced PEO/PVP blend for optoelectronic and energy storage devices, *Ceramics International* **49** (2023) 18322-18333. https://doi.org/10.1016/j.ceramint.2023.02.204

[12] J. Sugumaran, A. L. Ahmada, N. D. Zaulkiflee, Improvement of ionic conductivity of titanium dioxide incorporated PVDF-HFP/cellulose acetate electrolyte membrane, *IOP Conference Series: Materials Science and Engineering* **736** (2020) 052025. https://doi.org/10.1088/1757-899X/736/5/052025

[13] H. T. Ahmed, O.G. Abdullah, Preparation and Composition Optimization of PEO:MC Polymer Blend Films to Enhance Electrical Conductivity, *Polymers* **11** (2019) 853. https://doi.org/10.3390/polym11050853

[14] S. A. Rasaki, C. Liu, C. Lao, Z. Chen, A review of current performance of rare earth metal-doped barium zirconate perovskite: The promising electrode and electrolyte material for the protonic ceramic fuel cells, *Progress in Solid State Chemistry* **63** (2021) 100325. https://doi.org/10.1016/j.progsolidstchem.2021.100325

[15] A. Jagadeesan, M. Sasikumar, R. Hari Krishna, N. Raja, D. Gopalakrishna, S. Vijayashree, P. Sivakumar, High electrochemical performance of nano TiO_2 ceramic filler incorporated PVC-PEMA composite gel polymer electrolyte for Li-ion battery applications, *Materials Research Express* **6** (2019) 105524. https://doi.org/10.1088/2053-1591/ab3cb8

[16] B. Luo, W. Wang, Q. Wang, W. Ji, G. Yu, Z. Liu, Z. Zhao, X. Wang, S. Wang, J. Zhang, Facilitating ionic conductivity and interfacial stability *via* oxygen vacancies-enriched TiO_2 microrods for composite polymer electrolytes, *Chemical Engineering Journal* **460** (2023) 141329. https://doi.org/10.1016/j.cej.2023.141329

[17] K. Deshmukh, M. Basheer Ahamed, R. R. Deshmukh, S. K. Khadheer Pasha, P. R. Bhagat, K. Chidambaram, *Biopolymer Composites With High Dielectric Performance: Interface Engineering*, in: *Biopolymer Composites Electronics*, Elsevier, 2017, pp. 27-128. https://doi.org/10.1016/B978-0-12-809261-3.00003-6

[18] L. Ma, T. Shi, Z. Zhang, X. Liu, H. Wang, Wettability of HPMC/PEG/CS Thermosensitive Porous Hydrogels, *Gels* **9** (2023) 667. https://doi.org/10.3390/gels9080667

[19] P. Zarrintaj, M. R. Saeb, S. H. Jafari, M. Mozafari, *Application of compatibilized polymer blends in biomedical fields*, in: Compatilization of Polymer Blends, Elsevier, 2020, pp. 511-537. https://doi.org/10.1016/B978-0-12-816006-0.00018-9

[20] A. A. Al-Muntaser, R. A. Pashameah, A. Saeed, R. Alwafi, E. Alzahrani, S. A. AlSubhi, A. Y. Yassin, Boosting the optical, structural, electrical, and dielectric properties of polystyrene using a hybrid GNP/Cu nanofiller: novel nanocomposites for energy storage applications, *Journal of Materials Science: Materials in Electronics* **34** (2023) 678. https://doi.org/10.1007/s10854-023-10104-7

[21] L. Zhang, J. Lian, L. Wu, Z. Duan, J. Jiang, L. Zhao, Synthesis of a Thin-Layer MnO 2 Nanosheet-Coated Fe 3 O 4 Nanocomposite as a Magnetically Separable Photocatalyst, *Langmuir* **30** (2014) 7006-7013. https://doi.org/10.1021/la500726v

[22] M. Sasikumar, R. H. Krishna, M. Raja, H. A. Therese, N. T. M. Balakrishnan, P. Raghavan, P. Sivakumar, Titanium dioxide nano-ceramic filler in solid polymer electrolytes: Strategy towards suppressed dendrite formation and enhanced electrochemical performance for safe lithium ion batteries, *Journal of Alloys and Compounds* **882** (2021) 160709. https://doi.org/10.1016/j.jallcom.2021.160709

[23] C. Li, Y. Huang, C. Chen, X. Feng, Z. Zhang, High-performance polymer electrolyte membrane modified with isocyanate-grafted Ti^{3+} doped TiO_2 nanowires for lithium batteries, *Applied Surface Science* **563** (2021) 150248. https://doi.org/10.1016/j.apsusc.2021.150248

[24] N. Ramaiah, V. Raja, C. Ramu, Preparation and characterisation of electrolyte filled solid poly (vinylidene difluoride-co-hexafluoropropylene) polymer TiO_2 membranes for battery application, *Materials Research Innovations* **26** (2022) 214-221. https://doi.org/10.1080/14328917.2021.1942406

[25] J. C. Barbosa, R. Gonçalves, C. M. Costa, S. Lanceros-Méndez, Toward Sustainable Solid Polymer Electrolytes for Lithium-Ion Batteries, *ACS Omega* **7** (2022) 14457-14464. https://doi.org/10.1021/acsomega.2c01926

[26] N. Farah, H. M. Ng, A. Numan, C.-W. Liew, N. A. A. Latip, K. Ramesh, S. Ramesh, Solid polymer electrolytes based on poly(vinyl alcohol) incorporated with sodium salt and ionic liquid for electrical double layer capacitor, *Materials Science and Engineering: B* **251** (2019) 114468. https://doi.org/10.1016/j.mseb.2019.114468

[27] M. Grześkowiak, R. J. Wróbel, J. Grzechulska, J. Przepiórski, Preparation and characterization of titania powders obtained via hydrolysis of titanium tetraisopropoxide, *Materials Science-Poland* **32** (2014) 71-79. https://doi.org/10.2478/s13536-013-0163-z

[28] S. Mahata, S.S. Mahato, M. M. Nandi, B. Mondal, *Synthesis of TiO_2 nanoparticles by hydrolysis and peptization of titanium isopropoxide solution*, *AIP Conference Proceedings* **1461(1)** (2012) 225-228. https://doi.org/10.1063/1.4736892

[29] L. Cano-Casanova, A. Amorós-Pérez, M. Ouzzine, M .A. Lillo-Ródenas, M.C. Román-Martínez, One step hydrothermal synthesis of TiO2 with variable HCl concentration: Detailed characterization and photocatalytic activity in propene oxidation, *Applied Catalysis B: Environmental* **220** (2018) 645-653. https://doi.org/10.1016/j.apcatb.2017.08.060

[30] S. Saravanan, M. Balamurugan, T. Soga, Synthesis of Titanium Dioxide Nanoparticles with Desired Ratio of Anatase and Rutile Phases and the Effect of High Temperature Annealing, *Transactions of the Materials Research Society of Japan* **43** (2018) 255-261. https://doi.org/10.14723/tmrsj.43.255

[31] D. Kida, O. Gładysz, M. Szulc, J. Zborowski, A. Junka, M. Janeczek, A. Lipińska, A. Skalec, B. Karolewicz, Development and Evaluation of a Polyvinylalcohol -Cellulose Derivative-Based Film with Povidone-Iodine Predicted for Wound Treatment, *Polymers* **12** (2020) 1271. https://doi.org/10.3390/polym12061271

[32] M. Sahu, V. R. M. Reddy, B. Kim, B. Patro, C. Park, W. K. Kim, P. Sharma, Fabrication of Cu_2ZnSnS_4 Light Absorber Using a Cost-Effective Mechanochemical Method for Photovoltaic Applications, *Materials* **15** (2022) 1708. https://doi.org/10.3390/ma15051708

[33] S. E. Bianchi, V .W. Angeli, K. C. B. de Souza, D. dos S. Miron, G. de A. Carvalho, V. dos Santos, R.N . Brandalise, Evaluation of the solubility of the HPMC: PVA blends in biological fluids in vitro, *Materials Research* **14** (2011) 166-171. https://doi.org/10.1590/S1516-14392011005000033

[34] Ri. Prasanna, Ku. Sankari, Design, evaluation and in vitro - in vivo correlation of glibenclamide buccoadhesive films, *International Journal of Pharmaceutical Investigation* **2** (2012) 26. https://doi.org/10.4103/2230-973X.96923

[35] S. Abbad, K. Guergouri, S. Gazaout, S. Djebabra, A. Zertal, R. Barille, M. Zaabat, Effect of silver doping on the photocatalytic activity of TiO_2 nanopowders synthesized by the sol-gel route, *Journal of Environmental Chemical Engineering* **8** (2020) 103718. https://doi.org/10.1016/j.jece.2020.103718

[36] H. T. Ahmed, V. J. Jalal, D. A. Tahir, A. H. Mohamad, O. G. Abdullah, Effect of PEG as a plasticizer on the electrical and optical properties of polymer blend electrolyte MC-CH-$LiBF_4$ based films, *Results in Physics* **15** (2019) 102735. https://doi.org/10.1016/j.rinp.2019.102735

[37] Harshlata, K. Mishra, D.K. Rai, Effect of polymer blending on the electrochemical properties of porous PVDF/PMMA membrane immobilized with organic solvent based liquid electrolyte, *International Journal of Materials Research* **114** (2023) 662-670. https://doi.org/10.1515/ijmr-2021-8758

[38] A.K. Chauhan, D. Kumar, K. Mishra, A. Singh, Performance enhancement of Na^+ ion conducting porous gel polymer electrolyte using $NaAlO_2$ active filler, *Materials Today Communications* **26** (2021) 101713. https://doi.org/10.1016/j.mtcomm.2020.101713

[39] S. B. Aziz, E. M. A. Dannoun, M. H. Hamsan, H.O. Ghareeb, M. M. Nofal, W. O. Karim, A. S .F. M. Asnawi, J. M. Hadi, M. F. Z. A. Kadir, A Polymer Blend Electrolyte Based on CS with Enhanced Ion Transport and Electrochemical Properties for Electrical Double Layer Capacitor Applications, *Polymers* **13** (2021) 930. https://doi.org/10.3390/polym13060930

[40] E. Trevisanello, T. Ates, S. Passerini, F.H. Richter, J. Janek, Influence of the Polymer Structure and its Crystallization on the Interface Resistance in Polymer-LATP and Polymer-LLZO Hybrid Electrolytes, *Journal of The Electrochemical Society* **169** (2022) 110547. https://doi.org/10.1149/1945-7111/aca125

[41] M. Ravi, K. Kiran Kumar, V. Madhu Mohan, V.V.R. Narasimha Rao, Effect of nano TiO_2 filler on the structural and electrical properties of PVP based polymer electrolyte films, *Polymer Testing* **33** (2014) 152-160. https://doi.org/10.1016/j.polymertesting.2013.12.002

[42] W. Zhai, Y. Zhang, L. Wang, F. Cai, X. Liu, Y. Shi, H. Yang, Study of nano-TiO_2 composite polymer electrolyte incorporating ionic liquid PP12O1TFSI for lithium battery, *Solid State Ionics* **286** (2016) 111-116. https://doi.org/10.1016/j.ssi.2016.01.019

[43] J. Yang, X. J. Meng, M. R. Shen, L. Fang, J. L. Wang, T. Lin, J. L. Sun, J. H. Chu, Hopping conduction and low-frequency dielectric relaxation in 5 mol% Mn doped (Pb,Sr)TiO_3 films, *Journal of Applied Physics* **104** (2008) 104113. https://doi.org/10.1063/1.3021447

[44] X. Wang, H. Zhai, B. Qie, Q. Cheng, A. Li, J. Borovilas, B. Xu, C. Shi, T. Jin, X. Liao, Y. Li, X. He, S. Du, Y. Fu, M. Dontigny, K. Zaghib, Y. Yang, Rechargeable solid-state lithium metal batteries with vertically aligned ceramic nanoparticle/polymer composite electrolyte, *Nano Energy* **60** (2019) 205-212. https://doi.org/10.1016/j.nanoen.2019.03.051

[45] S. A. Ahmed, T. Pareek, S. Dwivedi, M. Badole, S. Kumar, $LiSn_2(PO_4)_3$-based polymer-in-ceramic composite electrolyte with high ionic conductivity for all-solid-state lithium batteries, *Journal of Solid State Electrochemistry* **24** (2020) 2407-2417. https://doi.org/10.1007/s10008-020-04783-z

[46] X. Mei, Y. Wu, Y. Gao, Y. Zhu, S.-H. Bo, Y. Guo, A quantitative correlation between macromolecular crystallinity and ionic conductivity in polymer-ceramic composite solid electrolytes, *Materials Today Communications* **24** (2020) 101004. https://doi.org/10.1016/j.mtcomm.2020.101004

[47] R. Deivanayagam, M. Cheng, M. Wang, V. Vasudevan, T. Foroozan, N. V. Medhekar, R. Shahbazian-Yassar, Composite Polymer Electrolyte for Highly Cyclable Room-Temperature Solid-State Magnesium Batteries, *ACS Applied Energy Materials* **2** (2019) 7980-7990. https://doi.org/10.1021/acsaem.9b01455

[48] X. Hu, M. Jing, H. Yang, Q. Liu, F. Chen, W. Yuan, L. Kang, D. Li, X. Shen, Enhanced ionic conductivity and lithium dendrite suppression of polymer solid electrolytes by alumina nanorods and interfacial graphite modification, *Journal of Colloid and Interface Science* **590** (2021) 50-59. https://doi.org/10.1016/j.jcis.2021.01.018

[49] T. Pareek, S. Dwivedi, S.A. Ahmad, M. Badole, S. Kumar, Effect of NASICON-type $LiSnZr(PO4)_3$ ceramic filler on the ionic conductivity and electrochemical behavior of PVDF based composite electrolyte, *Journal of Alloys and Compounds* **824** (2020) 153991. https://doi.org/10.1016/j.jallcom.2020.153991

[50] B. Liu, Y. Huang, H. Cao, L. Zhao, Y. Huang, A. Song, Y. Lin, X. Li, M. Wang, A novel porous gel polymer electrolyte based on poly(acrylonitrile-polyhedral oligomeric silsesquioxane) with high performances for lithium-ion batteries, *Journal of Membrane Science* **545** (2018) 140-149. https://doi.org/10.1016/j.memsci.2017.09.077

[51] A. Song, Y. Huang, X. Zhong, H. Cao, B. Liu, Y. Lin, M. Wang, X. Li, Novel lignocellulose based gel polymer electrolyte with higher comprehensive performances for rechargeable lithium-sulfur battery, *Journal of Membrane Science* **556** (2018) 203-213. https://doi.org/10.1016/j.memsci.2018.04.003